Cyclic Prefix Based Symbol Timing Synchronization Method for OFDM Systems by Using the Correlation Property of Preamble

Chong Wang and Junghwan Kim
EECS Dept. The University of Toledo, Toledo, OH 43606
jkim@utnet.utoledo.edu

***Abstract*—In this paper, an improved and effective estimation method for orthogonal frequency division multiplexing (OFDM) symbol timing synchronization is proposed. This maximum likelihood estimation (MLE) based method takes advantage of (cyclic prefix) CP along with the conventional training sequence, which consists of four identical parts (but the last two parts with different sign). By exploring the multivariate Gaussian distribution within the OFDM preamble symbol as well as corresponding CP, the accuracy of symbol timing error estimation can be significantly enhanced due to its smaller estimation variance. The performance of the proposed method is validated and compared with existing estimation (and synchronization) methods in terms of timing metric and mean square error (MSE) under AWGN, Rayleigh flat fading and frequency-selective multipath Rayleigh fading environments, respectively. Computer simulation results confirm the effectiveness of the proposed method under various levels of signal to noise ratio (SNR).**

Keywords- OFDM, synchronization, symbol timing error , mean square error (MSE), multivariate Gaussian distribution

I. INTRODUCTION

Orthogonal frequency division multiplexing (OFDM) modulation technique is widely utilized in various applications of mobile radio and digital audio broadcasting [1, 2]. However, despite its high spectral efficiency and low sensitivity to impulse noise and multipath fading [2], OFDM is sensitive to synchronization errors (symbol timing error and carrier frequency offset), which eventually result in inter-symbol interference (ISI) and inter-carrier interference (ICI). Although inserting cyclic prefix (CP) can alleviate ISI, symbol timing error still causes the phase rotation of the sub-carriers in frequency domain even if symbol timing error is shorter than the CP duration.

For an accurate estimation of symbol timing error, multiple efficient synchronization (and/or estimation) methods are currently available [3-8]. Schmidl and Cox [4] presented a data-aided (DA) method using a preamble with two identical halves for joint symbol timing and carrier frequency synchronization. But its timing metric exhibits a 'plateau' [4] for the whole duration of the CP, which inevitably yields large estimation variance. Later Minn [5, 6] proposed a modified method [6] in which Schmidl and Cox's [4] timing metric is averaged over a window of CP length to reduce the variance. Although this method can partially alleviate the 'plateau problem' of [4], the estimation variance is still large due to the comparable timing metric around the optimum timing. Minn also proposed another method [6] using the modified preamble sequence of [4], which contains four equal parts (but the last two parts with different sign). This method can yield relatively smaller estimator variance but it exhibits large mean square error (MSE) under multipath fading [6].

In this paper, we propose an improved synchronization method to estimate the symbol timing for OFDM systems. This maximum likelihood estimation (MLE) based method takes the effect of CP into consideration along with the conventional training sequence of Minn [6] toward compact timing error and minimum MSE. The proposed method is thoroughly evaluated and its performance is compared with existing DA synchronization algorithms (Schmidl [4], Minn1, and Minn2 [6]) in terms of the timing metric and MSE. The proposed method is derived under additive white Gaussian noise (AWGN), but it is also evaluated under frequency flat and frequency selective multipath Rayleigh fading as shown in Section IV. The corresponding computer simulation results confirm that the proposed algorithm yields the lowest MSE compared with those of the existing methods under AWGN, Rayleigh flat and frequency selective multipath fadings.

II. OFDM SYNCHRONIZATION

In OFDM systems, N_u complex data symbols are modulated into N subcarriers by using the inverse Fourier transform (IFFT) on the transmitter side, and the last L samples of the body of OFDM symbol are copied. They are appended as a CP to form a guard interval (GI), which is inserted at the beginning of each OFDM symbol, to generate the complete OFDM symbol. Hence, the effective length of the transmitted OFDM symbol is the CP plus the body length (total $N+L$ samples). The samples of the transmitted baseband OFDM signal, assuming ideal Nyquist pulse shaping, can be expressed as ($-L \le k \le N-1$),

$$s(k) = \frac{1}{\sqrt{N}} \sum_{n=0}^{N_u-1} C_n \exp(j\frac{2\pi}{N} kn) \qquad (1)$$

where C_n is the modulated subcarrier symbol. The received signals may additionally experience carrier frequency offset and symbol timing error. Let θ be the symbol timing error (in the unit of sample) and ε denotes the frequency offset normalized to the subcarrier spacing. Then, the received signal can be expressed as,

978-1-4673-1881-5/12/$31.00 ©2012 IEEE

$$r(k) = s(k-\theta)\exp(j\frac{2\pi}{N}\varepsilon k) + n(k) \quad (2)$$

where $n(k)$ denotes the complex AWGN. The goal of OFDM symbol timing is to estimate θ in the presence of ε, since most frequency offset estimation algorithm requires no symbol timing error. Thus, the symbol timing error estimation algorithm should be tolerant to the frequency offset.

III. Proposed Method

A. Preamble Sequence and Its Property

In this paper, the conventional preamble sequences (of Minn's) is selected, which is in the form of $T_{Minn} = [B_{N/4}, B_{N/4}, -B_{N/4}, -B_{N/4}]$ ($B_{N/4}$ denotes length $N/4$ complex samples of preamble sequence generated by taking $N/4$ points IFFT of $N/4$ modulated data) [6]. Let's assume that the transmitted signal is affected by complex AWGN only. The transmitted signal $s(k)$ in each identical part of the preamble (denoted by $B_{N/4}$) is a linear combination of independent, identically distributed random variables. Fig. 1 depicts the structures of OFDM signal with CP including the preamble sequence in the time domain, which is used in the proposed method. A length of $2N+L$ observation interval is used as in [7]. If θ is the symbol timing error in the units of samples, this observation interval can be divided into multiple smaller subsets of samples as shown in Fig. 1, which can be considered as a modified form of Minn's [6] preamble.

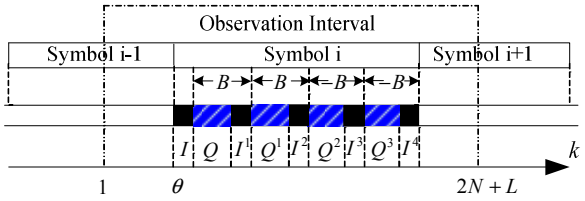

Figure 1. Structure of the Modified Minn's Preamble.

In Fig. 1, the set I denotes the CP copied from set I^4. Because the preamble sequence contains four correlated parts, set I has its correlated sample indices as sets I^1, I^2, I^3, I^4. Similarly, set Q also has the correlated sample indices as sets Q^1, Q^2, Q^3.

If the received signal in the observation interval is defined as $\vec{r} = [r(1), r(2), \ldots, r(2N+1)]^T$, only the samples in the union set C have their correlated parts. Where C is defined as $C = I \cup I^1 \cup I^2 \cup I^3 \cup I^4 \cup Q \cup Q^1 \cup Q^2 \cup Q^3$, thus,

$$\forall k \in I: E\{r(k)r^*(k+m)\} = \begin{cases} \sigma_s^2 + \sigma_n^2 & m = 0 \\ \sigma_s^2 e^{-j\pi\varepsilon/2} & m = N/4 \\ \sigma_s^2 e^{-j\pi\varepsilon} & m = N/2 \\ \sigma_s^2 e^{-j3\pi\varepsilon/2} & m = 3N/4 \\ \sigma_s^2 e^{-j2\pi\varepsilon} & m = N \\ 0 & otherwise \end{cases} \quad (3)$$

$$\forall k \in Q: E\{r(k)r^*(k+m)\} = \begin{cases} \sigma_s^2 + \sigma_n^2 & m = 0 \\ \sigma_s^2 e^{-j\pi\varepsilon/2} & m = N/4 \\ \sigma_s^2 e^{-j\pi\varepsilon} & m = N/2 \\ \sigma_s^2 e^{-j3\pi\varepsilon/2} & m = 3N/4 \\ 0 & otherwise \end{cases} \quad (4)$$

where $\sigma^2_s = E\{|s(k)|^2\}$ and $\sigma^2_n = E\{|n(k)|^2\}$. If the number of subcarriers is sufficiently large, each identical parts of the transmitted preamble can then be approximated as a complex Gaussian process, and its real and imaginary components are independent from each other. Then, the signal to noise ratio (SNR) can be defined as $SNR = \sigma^2_s/\sigma^2_n$.

B. Proposed Symbol Timing Synchronization Method

Let us define the log-likelihood function, $\Lambda(\theta, \varepsilon)$, which is the logarithm of the probability density function (pdf) $f(\vec{r})$ of the observed samples in received signal $\vec{r}$ on the condition of given symbol timing error θ,

$$\Lambda(\theta, \varepsilon) = \log[f(\vec{r} \mid \theta, \varepsilon)] \quad (5)$$

Then, using the correlation properties of the observations in the received signal, the log-likelihood function can be written as (6) (shown at the top of the next page), where $f(\,)$ denotes the pdf. Note that the third term in (6) is independent of θ and ε, and the numerators of the first and the second terms in (6) are in the form of 5-dimensional (5-D) and 4-D complex Gaussian distributions, respectively. From the multivariate Gaussian distribution, the joint pdf of the Gaussian random variable $f(\vec{r}_1) = f[r(k), r(k+N/4), r(k+N/2), r(k+3N/4)]$ is defined as [9],

$$f(\vec{r}_1) = A\exp[-\frac{1}{2}(\vec{r}_1 - \vec{m}_x)^T M^{-1}(\vec{r}_1 - \vec{m}_x)] \quad (7)$$

where A is constant value, $\vec{m}_x$ denotes the mean of these Gaussian distributed variables, M is the covariance matrix and its inverse matrix (M^{-1}) can be derived as in (8) (shown at the top of the next page). Then the joint pdf of the Gaussian random variable $\vec{r}_1$ can be calculated as (9), where

$$\rho = \left|\frac{E[(r(k)r^*(k+\frac{N}{2})]}{\sigma_s^2 + \sigma_n^2}\right| = \frac{\sigma_s^2}{\sigma_s^2 + \sigma_n^2} = \frac{SNR}{SNR+1} \quad (10)$$

Hence, the ML estimate of the second term in (6) can be derived as in (11) ((9) and (11) are shown at the top of the 4th page), where m_i is $\pi\varepsilon/2$, $\pi\varepsilon$, $3\pi\varepsilon/2$, $\pi\varepsilon$, $\pi\varepsilon/2$, and $\pi\varepsilon/2$ for i from 1 to 6, the symbol '$\propto$' denotes "proportional to", and

$$\gamma_1(\theta) = \sum_{k=\theta+L}^{\theta+N/4-1} r(k)r^*(k+N/4)$$

$$\phi_1(\theta) = \frac{1}{2}\sum_{k=\theta+L}^{\theta+N/4-1} |r(k)|^2 + |r(k+N/4)|^2$$

$$\Lambda(\theta,\varepsilon)=\log\{\prod_{k\in I}\frac{f[r(k),r(k+\frac{N}{4}),r(k+\frac{N}{2}),r(k+\frac{3N}{4}),r(k+N]}{f[r(k)]f[r(k+\frac{N}{4})]f[r(k+\frac{N}{2})]f[r(k+\frac{3N}{4})]f[r(k+N)]}$$

$$\prod_{k\in Q}\frac{f[r(k),r(k+\frac{N}{4}),r(k+\frac{N}{2}),r(k+\frac{3N}{4})]}{f[r(k)]f[r(k+\frac{N}{4})]f[r(k+\frac{N}{2})]f[r(k+\frac{3N}{4})]}\prod_{k}f[r(k)]\} \quad (6)$$

$$M^{-1}=\frac{1}{(\sigma_s^2+\sigma_n^2)(2\rho-3\rho^2+1)}\begin{bmatrix}2\rho+1 & -\rho & -\rho & -\rho\\ -\rho & 2\rho+1 & -\rho & -\rho\\ -\rho & -\rho & 2\rho+1 & -\rho\\ -\rho & -\rho & -\rho & 2\rho+1\end{bmatrix} \quad (8)$$

$$\gamma_2(\theta)=\sum_{k=\theta+L}^{\theta+N/4-1}r(k)r^*(k+N/2)$$

$$\phi_2(\theta)=\frac{1}{2}\sum_{k=\theta+L}^{\theta+N/4-1}\left|r(k)\right|^2+\left|r(k+N/2)\right|^2$$

$$\gamma_3(\theta)=\sum_{k=\theta+L}^{\theta+N/4-1}r(k)r^*(k+3N/4)$$

$$\phi_3(\theta)=\frac{1}{2}\sum_{k=\theta+L}^{\theta+N/4-1}\left|r(k)\right|^2+\left|r(k+3N/4)\right|^2$$

$$\gamma_4(\theta)=\sum_{k=\theta+L}^{\theta+N/4-1}r(k+N/4)r^*(k+N/2)$$

$$\phi_4(\theta)=\frac{1}{2}\sum_{k=\theta+L}^{\theta+N/4-1}\left|r(k+N/4)\right|^2+\left|r(k+N/2)\right|^2$$

$$\gamma_5(\theta)=\sum_{k=\theta+L}^{\theta+N/4-1}r(k+N/4)r^*(k+3N/4)$$

$$\phi_5(\theta)=\frac{1}{2}\sum_{k=\theta+L}^{\theta+N/4-1}\left|r(k+N/4)\right|^2+\left|r(k+3N/4)\right|^2$$

$$\gamma_6(\theta)=\sum_{k=\theta+L}^{\theta+N/4-1}r(k+3N/4)r^*(k+N)$$

$$\phi_6(\theta)=\frac{1}{2}\sum_{k=\theta+L}^{\theta+N/4-1}\left|r(k+3N/4)\right|^2+\left|r(k+N)\right|^2$$

The maximum value of (11) with respect to the frequency offset is obtained when the cosine term in (11) equals to one [7]. As can be seen from above equations, the phases of $\angle\gamma_i(\theta)$ are approximately equal to m_i at the optimum timing point simultaneously. Thus, $\cos(m_i\varepsilon+\angle\gamma_i(\theta))\approx 1$ for all i from 1 to 6 in (11). Similarly, the first term of (6) is a 5-D case. Using the multivariate Gaussian distribution, the ML estimate of first term in (6) can be calculated as (12) (shown at the top of the next page). Since the definitions of $\alpha_i(\theta)$ and $\beta_i(\theta)$ are straightforward and can be easily obtained as $\gamma_i(\theta)$ and $\phi_i(\theta)$ in (11), they are not given here due to lack of space. Hence, the corresponding ML timing metric becomes,

$$M_{proposed}=\sum_{i=1}^{6}\left[\left|\gamma_i(\theta)\right|-\rho\phi_i(\theta)\right]+\sum_{i=1}^{10}\left[\left|\alpha_i(\theta)\right|-\rho\beta_i(\theta)\right] \quad (13)$$

IV. Simulation Environment And Results

For an effective validation of the proposed symbol timing error estimation method, performances are evaluated via computer simulations using timing metric and MSE of the error estimator. Results are then compared with Schmidl's [4] and Minn's [6], exploring the degrading effects under AWGN, Rayleigh flat fading and frequency selective fading, respectively. Table I shows the simulation parameters based on the wireless IEEE 802.11a standard [10]. Note that the carrier frequency offset ε is assumed to be 5% of the subcarrier spacing for all cases.

TABLE I. Simulation Parameters for OFDM Systems Based on IEEE 802.11A Standard

FFT size N	64
Number of data subcarriers N_d	48
Number of pilot subcarriers N_p	4
Number of subcarriers $N_u=N_d+N_p$	52
OFDM data symbol duration T	3.2 us
Subcarrier spacing $1/T$	0.3125 MHz
Sampling frequency N/T	20 MHz
Guard interval	$T/8$
Modulation scheme	QPSK

Fig. 2 shows the timing metrics without noise and channel distortion. The correct symbol timing is indexed as 0 in the figure. The timing metric of the proposed method (curve 1) is compared with those of Schmidl's and Minn's. In Fig. 3, Schmidl's metric (curve 2) creates a 'plateau' for the whole interval of CP. The timing metric of Minn1 method (curve 3) effectively reduces the size of this plateau, but still yields comparable metric values around the correct timing metric. While metric of Minn2 (curve 4) exhibits relatively better

$$f(\vec{r}_1) = A\exp[-\frac{1}{2(\sigma_s^2+\sigma_n^2)(2\rho-3\rho^2+1)}\{(2\rho+1)|r(k)|^2+(2\rho+1)|r(k+N/4)|^2$$
$$+(2\rho+1)|r(k+N/2)|^2+(2\rho+1)|r(k+3N/4)|^2-2\rho\,\mathrm{Re}[e^{j\pi\varepsilon/2}r(k)r^*(k+N/4)]$$
$$-2\rho\,\mathrm{Re}[e^{j\pi\varepsilon}r(k)r^*(k+N/2)]-2\rho\,\mathrm{Re}[e^{j\pi 3\varepsilon/4}r(k)r^*(k+3N/4)]$$
$$-2\rho\,\mathrm{Re}[e^{j\pi\varepsilon/2}r(k+N/4)r^*(k+N/2)]-2\rho\,\mathrm{Re}[e^{j\pi\varepsilon}r(k+N/4)r^*(k+3N/4)]$$
$$-2\rho\,\mathrm{Re}[e^{j\pi\varepsilon/2}r(k+N/4)r^*(k+N/2)]\} \quad (9)$$

$$\prod_{k\in Q}\frac{f[r(k),r(k+\frac{N}{4}),r(k+\frac{N}{2}),r(k+\frac{3N}{4})]}{f[r(k)]f[r(k+\frac{N}{4})]f[r(k+\frac{N}{2})]f[r(k+\frac{3N}{4})]}=\sum_{i=1}^{6}\left[|\gamma_i(\theta)|\cos(m_i\varepsilon+\angle\gamma_i(\theta))-\rho\phi_i(\theta)\right]\propto\sum_{i=1}^{6}\left[|\gamma_i(\theta)|-\rho\phi_i(\theta)\right] \quad (11)$$

$$\prod_{k\in I}\frac{f[r(k),r(k+\frac{N}{4}),r(k+\frac{N}{2}),r(k+\frac{3N}{4}),r(k+N]}{f[r(k)]f[r(k+\frac{N}{4})]f[r(k+\frac{N}{2})]f[r(k+\frac{3N}{4})]f[r(k+N)]}\propto\sum_{i=1}^{10}\left[|\alpha_i(\theta)|-\rho\beta_i(\theta)\right] \quad (12)$$

metric than those of Schmidl's and Minn1's, it still exhibits non-negligible peaks around correct timing. When comparing the proposed methods with other existing methods, the timing metric of the proposed methods exhibit very sharp peak value at the correct point with very small metric values around it, which can yield more accurate timing error estimation.

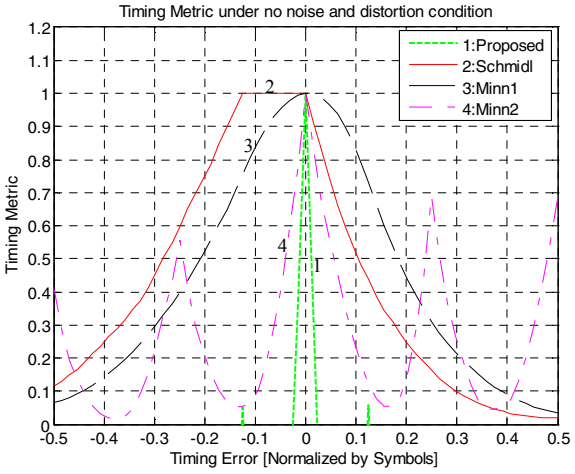

Figure 2. Comparison of Timing Metric of the Conventional and Proposed Estimators.

A. MSE Performance underAWGN

Fig. 3 shows the MSE of the symbol timing error estimators under AWGN. As can be seen from the Fig. 3, Minn1 method (curve 3) shows better performance than Schmidl method (curve 2), and the proposed method (curve 1) exhibits better performance than all the other methods. It implies and proves that reduction of the timing metric plateau can effectively improve the estimation performance. The degradation of Minn2 shown in Fig. 3 can be attributed to the comparably high sub-peak values of timing metrics (peaks other than index 0) around correcting timing (see Fig. 3).

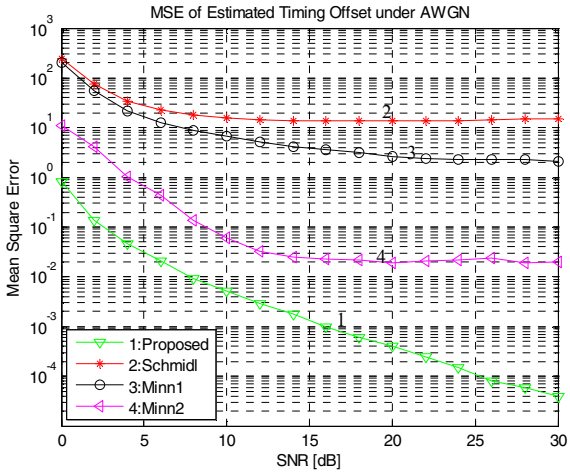

Figure 3. MSE of the Timing Offset Estimation under AWGN.

B. MSE Performance under Rayleigh Flat Fading

The received OFDM signal over a Rayleigh flat fading can be expressed as,

$$r(k) = hs(k-\theta)e^{j2\pi k\varepsilon/N}+n(k) \quad (14)$$

where h is Rayleigh fading variables. Because the proposed method is derived under AWGN, it cannot be directly applicable to this fading. To circumvent this difficulty, let's assume that: if P_h denotes the average power of h, the SNR can be rewritten as,

$$SNR = \sigma_s^2 P_h / \sigma_n^2 \quad (15)$$

Thus, the symbol timing estimation can be obtained by substituting (15) into (13). Fig. 4 shows the MSE performance of the estimators over Rayleigh flat fading. The simulation results clearly show the performance degradation caused by fading as compared with the corresponding curves for the

AWGN (compare the scale of MSE). Examining Fig. 4, the Minn2 method outperforms the Schmidl and Minn1 methods. Moreover, the proposed method shows better estimation accuracy than Minn2. Hence, the performance improvement of the proposed methods is verified.

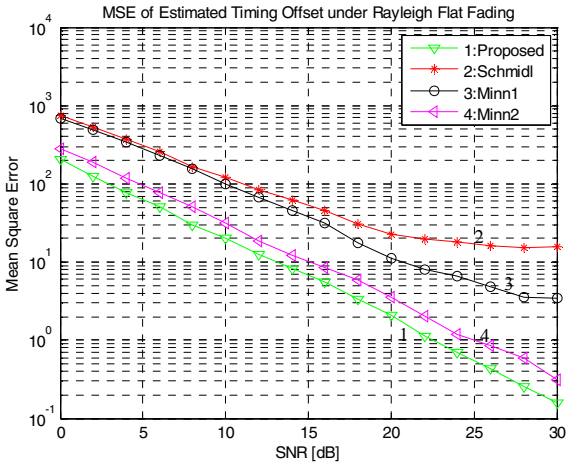

Figure 4. MSE of the Timing Offset Estimation under Rayleigh Flat Fading.

C. *MSE performance underRayleigh Frequency Selective Fading*

With regard to the frequency selective multi-path fading, a received OFDM signal can be expressed as,

$$r(k) = e^{j2\pi k\varepsilon/N}\sum_{l=0}^{D-1} h(l)s(k-\theta-l)+n(k) \qquad (16)$$

where D is number of transmission paths, and $h(l)$ is the channel impulse response with delay l. In our simulation, the frequency selective multipath Rayleigh fading has an exponentially decaying power delay profile with root mean squared width of 100 ns (corresponding to two samples), and the channel is modeled to simulate 5 independent paths with path delays of 0, 2, 4, 6, 8 samples. In this case, P_h is the sum of average power in all channels.

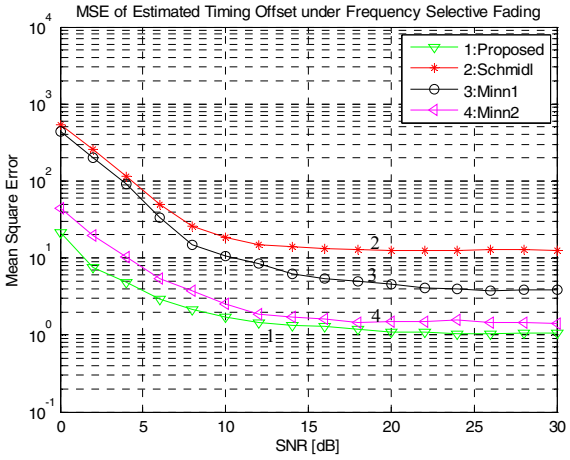

Figure 5. MSE of the Timing Offset Estimation under Rayleigh Frequency slective fading.

Fig. 5 shows the MSE of the estimators over Rayleigh frequency selective multipath fading channel. Since the CP is selected to consist of 8 samples, the ISI can be avoided. Examining the simulation results, the proposed method still outperforms the other algorithms under the whole SNR region.

Based on the simulation results exhibited in Figures 2 to 5, the proposed symbol timing estimator turns out to be quite effective and robust for the channel disturbances (AWGN and fading effects) due to its superior timing metric and minimum estimation MSE as to the symbol timing error.

V. CONCLUSIONS

In this paper, an improved MLE-based data aided symbol timing synchronization method has been presented for OFDM systems. This method uses the conventional training sequence with four identical halves as Minn [6], but it outperforms the existing algorithms [4-6] by exploiting the redundant information contained within the CP. Although it is mainly developed under the AWGN environment, it still can perform well even under frequency selective multipath Rayleigh fading. Extensive simulation results under various levels of SNRs confirm that the proposed estimation method is robust enough and can provide better performance in its estimation MSE than other estimators compared. Therefore, it can be a suitable choice for the synchronization of the OFDM system toward the applications of broadcast and wireless mobile.

REFERENCES

[1] Bo Ai, Zhi-xing Yang, Chang-yong Pan, Jian-hua Ge, and Yong Wang, Zhen Lu, "On the Synchronization Techniques for Wireless OFDM Systems," IEEE Trans. Broadcasting, vol. 52, no. 2, pp. 236-244, June 2006.

[2] A. Al-Dweik, A. Hazmi, S. Younis, B. Sharif, and C. Tsimenidis, "Carrier Frequency Offset Estimation for OFDM Systems Over Mobile Radio Channels," IEEE Trans. Vehicular Technology, vol. 59, no. 2, pp. 974-979, February 2010.

[3] Byungjoon Park, Eunseok Ko, Hyunsoo Cheon, Changeon Kang and Daesik Hong, "A blind OFDM Synchronization Algorithm Based on Cyclic Correlation," IEEE Trans. Signal Processing, vol. 11, no. 2, pp. 83-85, February 2004.

[4] T. M. Schmidl and D. C. Cox, "Robust Frequency and Timing Synchronization for OFDM," IEEE Trans. Commun., vol. 45, no. 12, pp. 1613-1621, December 1997.

[5] H. Minn, V. K. Bhargava, and K. B. Letaief, "A Robust Timing and Frequency Synchronization for OFDM systems," IEEE Trans. Wireless Commun., vol. 2, no. 4, pp. 822-839, July 2003.

[6] H. Minn, M. Zeng and V. K. Bhargava, "On Timing Offset Estimation for OFDM Systems," IEEE Trans. Wireless Commun., vol. 4, no. 7, pp. 242-244, July 2000

[7] J. J. van de Beek, M. Sandell, and P. O. Börjesson, "ML Estimation of Time and Frequency Offset in OFDM Systems," IEEE Trans. Signal Processing, vol. 45, no. 7, pp. 1800-1805, July 1997.

[8] D. Landström, S. K. Wilson, J. J. van de Beek, P. ödling and P. O. Börjesson, "Symbol Timing Offset Estimation in Coherent OFDM Systems," IEEE Trans. Commun., vol. 50, no. 4, pp. 545-549, April 2002.

[9] John G. Proakis, "Digital Communications," McGraw-Hill Science/Engineering/Math, 4th edition, pp. 48-51, August 15, 2000.

[10] "IEEE std 802.11a Part 11: Wireless LAN Medium Access Control (MAC) and Physical Layer (PHY) specifications High-speed Physical Layer in the 5 GHz Band," LAN/MAN Standards Committee of the IEEE Computer Society, 1999.